



PRECLINICAL IMAGING

Optimizing Injected Activity in Small-Animal In Vivo PET/CT & PET/MRI

Cesar Molinos, Todd Sasser. Nuclear Molecular Imaging, PCI, Bruker

Innovation with Integrity

Introduction

In small-animal PET, the injected tracer mass and activity should be determined by the biological application, rather than by tracer production yield, custom, or perceived scanner requirements. The key variables for defining the optimal tracer mass and activity are maintaining a mass consistent with the tracer principle and an absorbed dose that avoids deleterious biological effects. Nevertheless, there are reports in the literature of injected activities that contradict these requirements. This is likely due to the absence of standardized guidelines and the historical use of earlier-generation scanners, which required higher injected activities to achieve sufficient statistics for adequate image quality.

Modern high-sensitivity PET systems make it possible to obtain excellent image quality and robust quantitative data at activity levels well below the highest values reported in the literature. For a very narrow range of compounds and specific isotopes, higher injections (up to ~40 MBq, approximately 1100 μ Ci) may be warranted; however, in most cases, the more appropriate approach is to avoid unnecessarily high tracer mass and activity.

Tracer Activities in Preclinical PET Literature

In small-animal PET, there are no universally standardized protocols, so the activities reported in the specialized literature vary and depend strongly on acquisition duration, image analysis strategy, the biological application, and scanner sensitivity or count-rate capability. In many cases, reported activities per unit preclinical subject mass are many-fold higher than those reported per unit clinical patient mass. In some cases, activities per unit mass are more than 1000 \times higher in preclinical than in clinical use.

A scientific literature survey was conducted covering the most common small-animal in vivo PET applications. The activities reported in these studies are summarized below and in Table 1:

- **Oncology.** Mice were often studied using about 5 – 10 MBq (140 – 270 uCi) for common [18F] labeled tracers, whereas rats are more often in the 20 – 40+ MBq (approx. 540 – 1100 uCi) range, especially for dynamic or quantitative protocols. Dynamic kinetic studies and larger animals tend to push activity upward but exceeding 40 MBq is rare.
- **Neuro.** Mouse brain studies often used ~5 – 20 MBq (140 – 540 uCi) depending on whether the endpoint is metabolism, plaques, or functional brain imaging. Rat brain quantitative/metabolic studies were closer to ~48 MBq (1300 uCi), and receptor studies such as [11C]Raclopride can work in the single-digit to mid-teen MBq range. The main reported reasons are the need for dynamic quantification, the target biology (metabolism vs amyloid vs receptor availability), and whether imaging is whole-body or a small, dedicated brain field of view.
- **Cardiovascular.** In this application field doses are comparatively higher. The heart in both mice and rats is a small, moving, and the analysis may depend on very short dynamic or gated frames. The literature reports activities of 5 – 40 MBq (140 – 1100 uCi) in mice and 10 – 50 MBq (270 – 1400 uCi) in rats with the extreme case of ~70 MBq (1900 uCi) in some old ammonia-based cardiac studies in rats with legacy low sensitivity systems.

	Tracer	Mice	Rats	Selected References
Oncology	[18F]-FDG (Tumor metabolism)	5 – 10 MBq (140 – 270 uCi)	20-30 MBq (*) (540-810 uCi)	[2] to [6]
	[18F]-FLT, [18F]-FAZA (Proliferation)			
	[18F]-Miso (Hypoxia)			
Neuro	[18F]-FDG (cerebral metabolism)	10 – 20 MBq (270 – 540 uCi)	20-30 MBq (**) (810 – 540 uCi)	[7],[8]
	[18F]-Florbetaben (amyloid deposition in Alzheimer)			
	[11C]-Raclopride (Dopamine D2/D3 receptor imaging)	-	5 -20 MBq (140 – 540 uCi)	[9]
Cardiovascular	[18F]-FDG (cardiac function & myocardial metabolism)	5 – 40 MBq (140 – 1100 uCi)	10-50 MBq (270 – 1400 uCi)	[10]
	[13N]-Ammonia (Myocardial perfusion)			20-70 MBq (540 – 1900 uCi)

(*) Max.: 40 MBq in some Kinetic modeling of hypoxia and perfusion

(**) Max: 48 MBq kinetic modeling with arterial blood sampling

Table 1 Summary of reported injected PET tracer doses in mice and rats from the scientific literature, focusing on the most common applications.

Higher activities were often reported for dynamic protocols, especially in cardiovascular applications. High doses are commonly used when very short dynamic frames (a few seconds) are required during the first pass. Elevated injected activities are also reported in rat brain glucose-metabolism studies and in tumor perfusion or hypoxia studies that rely on long (up to 90-minute) dynamic acquisitions with arterial sampling for quantitative kinetic analysis.

Some myocardial perfusion experiments in rats used up to 70 MBq (1900 μ Ci) of [¹³N]ammonia to quantify tracer distribution and validate PET measurements against ex vivo reference data. It should be noted that one of the early examples of this application dates back to the late 1990s and employed a legacy system with a sensitivity of approximately 0.5–1%. Modern systems offer an order-of-magnitude higher sensitivity, and comparable tracer experiments have since been reported using injected activities as low as 20 MBq (540 μ Ci).

Tracer Principle and Clinical Systems

PET is built on the tracer principle: the administered compound should be present in sub-pharmacological amounts so that it reports biology without perturbing it. For receptor ligands in particular, the mass dose should be low enough to avoid meaningful target occupancy—guidance from quantitative PET references states that radioligand molecules should ideally occupy no more than about 1–5% of available receptor sites, because higher mass can occupy receptors and reduce target uptake, biasing binding estimates. This mass effect is especially important in small-animal PET.

In other applications, if we consider a typical [18F]-FDG procedure in a standard clinical PET system, a representative injected activity is about 370 MBq for an adult patient weighing 70 kg, corresponding to a specific activity of approximately 5.3 MBq/kg. By contrast, a 10 MBq injection (see Table 1.) in a 25 g mouse corresponds to about 400 MBq/kg.

Although this appears disproportionately high, activity normalized by body mass is not the only appropriate metric for comparing clinical and preclinical PET. A relevant consideration is the relationship between spatial resolution, object size, and system sensitivity. Preclinical PET systems achieve resolutions on the order of 1–2 mm, while clinical systems are typically in the 4–6 mm range. However, mouse organs are only a few millimeters in size, whereas human organs are several centimeters, meaning that small-animal imaging operates much closer to the resolution limit of the system. As a result, partial volume effects are more pronounced in preclinical imaging, reducing apparent activity concentrations and increasing noise, which in turn requires higher count density per unit volume to achieve sufficient image quality.

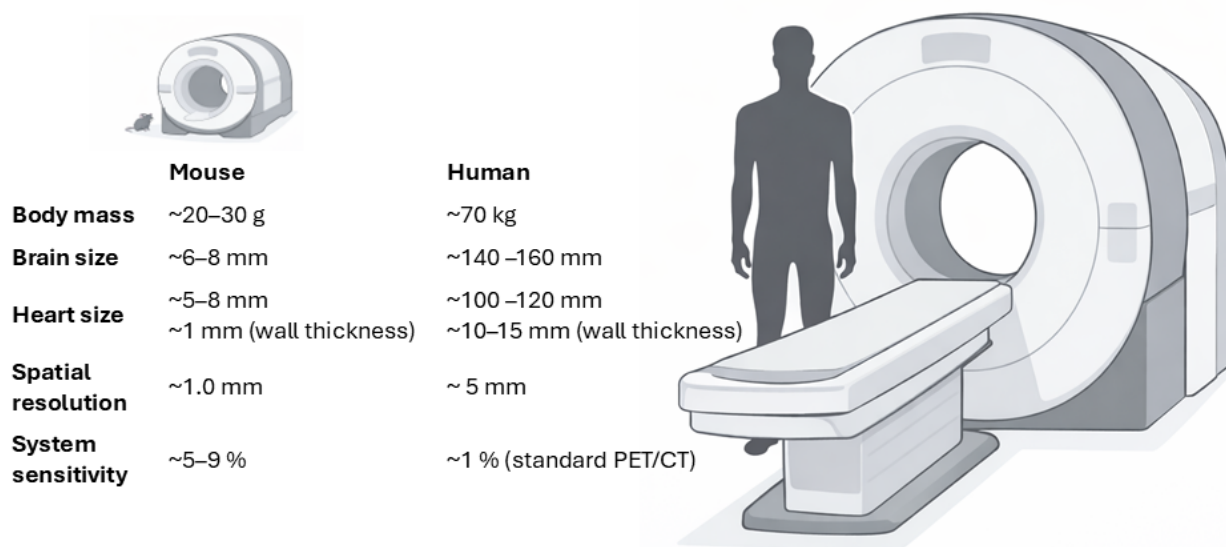


Figure 1 Comparison of typical clinical and preclinical PET dosing perspectives. When normalized to body mass, injected activities in preclinical PET can appear disproportionately high but partial volume effects are more pronounced in preclinical imaging due to the fact that animal organs have a size nearing the resolution of the scanner which requires higher counts per unit volume.

At the same time, preclinical PET systems typically offer substantially higher detection sensitivity than clinical scanners, which increases the number of detected events per unit activity. In principle, this improved sensitivity should enable a reduction in injected activity. However, in practice, the gains in sensitivity are partially offset by the need for higher spatial resolution and the associated increase in image noise at small voxel sizes. Consequently, while higher MBq/kg values in preclinical imaging can be partially explained by these competing factors, they likely exceed what is strictly necessary for a given imaging task.

Human Operator ALARA & 3Rs Animal Welfare

Higher injected activity increases the amount of radioactivity handled during dose drawing, syringe preparation, injection, and animal positioning. In routine [18F]-FDG PET practice, one study on technologist exposure reported mean whole-body doses of about 3 μ Sv per procedure, while finger doses during syringe preparation were much higher, reaching roughly 200 μ Sv per hand for multidose preparations. The same paper emphasizes that [18F]-FDG handling requires stronger radiation-protection measures because of the high-energy annihilation photons involved. Even though those measurements were obtained in clinical PET, the underlying lesson is directly relevant to preclinical work: the more activity handled, the greater the avoidable occupational exposure unless workflow, shielding, distance, and handling time are carefully optimized [12].

For the animal, the radiotracer injection is also a real source of radiation dose and should not be overlooked to comply with the modern standards of animal welfare like the 3Rs (Replacement, Reduction and Refinement) [13]. In a Monte Carlo simulation study of absorbed dose in a mouse phantom from [18F] compounds, simulations showed that a typical small-animal PET scan using [18F] tracers delivers whole-body absorbed doses on the order of tens of mGy (\approx 10–100 mGy, depending on injected activity and biodistribution), with particularly high doses to organs involved in tracer clearance such as the bladder. In contrast, a standard CT acquisition in mice usually delivers much lower doses, around \sim 1–10 mGy for routine anatomical imaging (though higher for high-resolution protocols). This means that, in

most small-animal PET/CT studies, the PET component dominates the total radiation burden—often by about an order of magnitude—while CT contributes a comparatively minor fraction unless aggressive imaging settings are used [14]. A more recent preclinical dosimetry study using [18F]-FDG in a mouse model reported a measured relationship between time-integrated activity and absorbed dose of 0.064 ± 0.06 Gy/MBq-h, demonstrating directly that the injected PET tracer contributes measurable internal dose to tissues. This is important because CT dose in longitudinal studies is often discussed explicitly, while the dose delivered by the PET injection itself may receive less attention in day-to-day protocol design. A sound dose strategy for small-animal PET must therefore consider both components: the x-ray burden from CT and the internal radiation burden from the radiotracer [15].

Deciding how much to inject

The guiding principle should be to use the lowest injected activity that provides the required quantitative precision for the planned scan duration, while keeping the injected chemical mass firmly within the tracer regime and the radiation burden as low as reasonably achievable. Recommendations from the scanner manufacturer should also be taken into account.

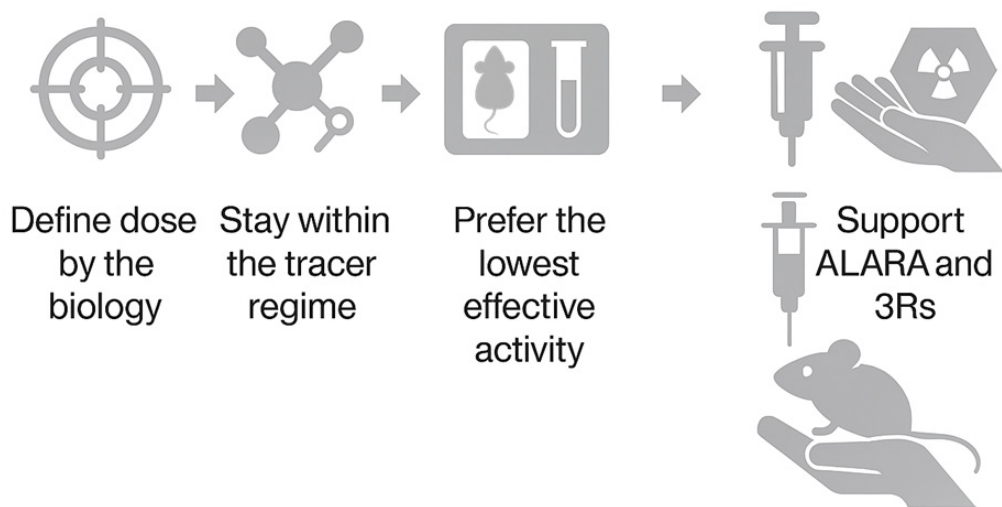


Figure 2 Conceptual summary of dose selection in small-animal PET. Injected activity should be determined by the biological question, tracer mass constraints, and the need for quantitative precision, while keeping radiation burden to animals and operators as low as reasonably achievable.

Although the NEMA Nu 4 2008 Noise Equivalent Count Rate (NECR) provides, for an specific experiment and object, an indication of the activity level beyond which additional activity no longer improves the signal to noise ratio (strictly speaking, $S^2/(S+N)$), it is not the most informative metric for injection planning. A more relevant parameter is the linear activity range, as it reflects count rates after correction for detector dead time. Ensuring linearity and accurate quantification across this range is what ultimately matters.

The [18F] linearity of the PET/CT Si78 and Bruker PET/MRI inserts is maintained up to approximately 40 MBq (1.1 mCi). The lower and upper limits of quantification accuracy for Bruker PET/CT Si78 and PET Inserts for PET/MRI are:

- 130 kBq to < 1.3 MBq: $\pm 10\%$
- 1.3 MBq to < 35 MBq: $\pm 5\%$
- 35 MBq to 40 MBq: $\pm 10\%$

Even for a given scanner, it is not possible to provide a single, specific recommendation that applies to all use cases, as animal size, tracer type, and acquisition duration vary widely. Nevertheless, it is still useful to provide a general recommendation for [18F] isotopes based on in-house experience and customer feedback. This can serve as a practical starting point when deciding how much activity to inject for other tracers and applications.

	Mice	Rats
Oncology	1 - 3 MBq (27 - 80 uCi)	5 - 10 MBq (140 - 270 uCi)
Neuro	3 - 5 MBq (80 - 140 uCi)	5 - 10 MBq (140 - 270 uCi)
Cardiovascular/Gated	5 - 10 MBq (140 - 270 uCi)	10 - 30 MBq (270 - 810 uCi)

Table 2 [18F]-FDG Injection Recommendation for the Bruker PET systems: PET/CT Si78 and PET Insert Si 103 and Insert Si 198.

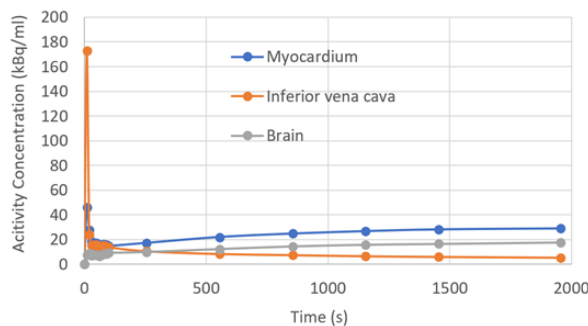
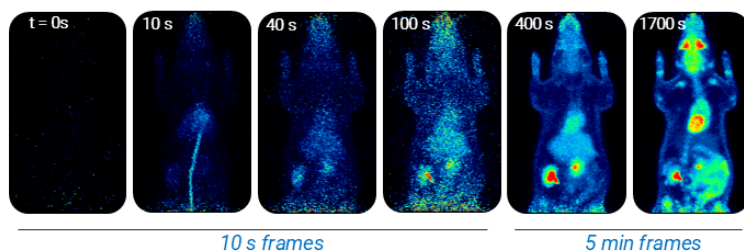


Figure 3 Dynamic PET imaging following a low-activity injection (3 MBq) of [18F]-FDG in a rat demonstrates the feasibility of quantitative analysis under low-dose conditions with the PET/CT Si78. The time–activity curves exhibit consistent and physiologically plausible kinetics in target organs such as the myocardium and brain. Despite the reduced administered activity, stable signal and reproducible uptake patterns are observed. The inferior vena cava shows a pronounced early peak and rapid washout, indicating that it can serve as a practical surrogate for the arterial input function in kinetic modeling. Representative images from early (10 s) and late (5 min) frames illustrate the temporal distribution of tracer and confirm sufficient image quality for dynamic analysis.



A useful way to help determine the appropriate injection dose for a given isotope is to evaluate scanner performance using a phantom. In particular, the NEMA IQ phantom can be used to assess image noise, recovery as a function of object size, and correction accuracy. Although tracer uptake in animals is more complex, phantom studies remain highly informative for expected image quality and for optimizing reconstruction settings.

Discussion

The central question in small-animal PET is not how much radioactivity a system can tolerate, but how much activity is genuinely required to obtain reliable results, safely and ethically. For [18F]-FDG, practical experience supports that approximately 1 to 3 MBq (80 uCi) in mice and about 5 to 10 MBq (140 - 270 uCi) in rats is sufficient for many standard in vivo PET studies when a modern, high-sensitivity system is used. Those values already provide a comfortable operating range for routine work while reducing unnecessary exposure to both staff and animals [16-20].

This philosophy becomes even more important in multi-animal imaging. If four mice are scanned simultaneously and each receives 10 MBq (270 uCi), the total activity in the field of view for a typical 4-mouse hotel is 40 MBq (1100 uCi). A system that can still quantify accurately under those realistic conditions already offers more than enough headroom for demanding day-to-day studies.

The relevant metric is not merely the ability to advertise tolerance to very high activity levels, but the ability to deliver robust, quantitative imaging across the activity range that is actually needed in a laboratory. Low dose dynamic imaging studies have shown that injections do not need to be high when quantification accuracy remains at low activity levels [16].

References:

1. Ribeiro, F.M., Correia, P.M.M., Santos, A.C. et al. A guideline proposal for mice preparation and care in [18F]-FDG PET imaging. *EJNMMI Res* 12, 49 (2022).
2. Melinda Wuest, Hans-Soenke Jans, Piyush Kumar, Leonard Wiebe and Alexander McEwan. Characterization of the murine EMT-6 tumor model with [18F]FDG, [18F]FLT and [18F]FAZA using dynamic small animal PET imaging. *Journal of Nuclear Medicine* May 2010, 51 (supplement 2) 1096.
3. Rick Wray, Audrey Mauguén, Laure Michaud, Doris Leithner, Randy Yeh, Nadeem Riaz, Rosna Mirtcheva, Eric Sherman, Richard Wong, John Humm, Nancy Lee and Heiko Schöder. Development of 18F-Fluoromisonidazole Hypoxia PET/CT Diagnostic Interpretation Criteria and Validation of Interreader Reliability, Reproducibility, and Performance. *Journal of Nuclear Medicine* October 2024, 65 (10) 1526-1532.
4. Kirsten Reeves, Patrick Song, Benjamin Larimer and Anna Sorace. [18F]-FMISO PET imaging of tumor hypoxia to predict and monitor response to checkpoint inhibitor therapy. *Journal of Nuclear Medicine* May 2020, 61 (supplement 1) 407.
5. Aren van Waarde, David C.P. Cobben, Albert J.H. Suurmeijer, Bram Maas, Willem Vaalburg, Erik F.J. de Vries, Pieter L. Jager, Harald J. Hoekstra and Philip H. Elsinga. Selectivity of 18F-FLT and [18F]-FDG for Differentiating Tumor from Inflammation in a Rodent Model. *Journal of Nuclear Medicine* April 2004, 45 (4) 695-700.
6. Eliane Weidl, Marion Menzel, Martin Janich, Oleksandr Khagai, Florian Wiesinger, Axel Haase, Stephan Nekolla, Rolf Schulte and Markus Schwaiger. In vivo detection of tumor metabolism with [18F]-FDG PET and hyperpolarized [1-13C]-pyruvate magnetic resonance spectroscopic imaging. *Journal of Nuclear Medicine* May 2012, 53 (supplement 1) 516.
7. Gregory D. Ayers, Allison S. Cohen, Seong-Woo Bae, Xiaoxia Wen, Alyssa Pollard, Shilpa Sharma, Trey Claus, Adria Payne, Ling Geng †, Ping Zhao, Mohammed Noor Tantawy, Seth T. Gammon, H. Charles Manning. Reproducibility and repeatability of 18F-(2S, 4R)-4-fluoroglutamine PET imaging in preclinical oncology models. Published: January 9, 2025.
8. Kazuaki Shimoji, Laura Ravasi, Kathleen Schmidt, Maria Luisa Soto-Montenegro, Takanori Esaki, Jurgen Seidel, Elaine Jagoda, Louis Sokoloff, Michael V. Green and William C. Measurement of Cerebral Glucose Metabolic Rates in the Anesthetized Rat by Dynamic Scanning with [18F]-FDG, the ATLAS Small Animal PET Scanner, and Arterial Blood Sampling Eckelman *Journal of Nuclear Medicine* April 2004, 45 (4) 665-672.
9. Bo Halle, Helge Thisgaard, Svend Hvidsten, Johan H. Dam, Charlotte Aaberg-Jessen, Anne S. Thykjær, Poul F. Høiland-Carlsen, Mette K. Schulz, Claus Andersen, and Bjarne W. Kristensen. Estimation of Tumor Volumes by 11C-MeAIB and [18F]-FDG PET in an Orthotopic Glioblastoma Rat Model. *J Nucl Med* 2015 Oct.
10. Michael C. Kreissl, Hsiao-Ming Wu, David B. Stout, Waldemar Ladno, Thomas H. Schindler, Xiaoli Zhang, John O. Prior, Mayumi L. Prins, Arion F. Chatziioannou, Sung-Cheng Huang and Heinrich R. Schelbert. Noninvasive Measurement of Cardiovascular Function in Mice with High-Temporal-Resolution Small-Animal PET. *Journal of Nuclear Medicine* June 2006, 47 (6) 974-980.
11. Takashi Kudo, MD; Kazuki Fukuchi, MD; Alexander J. Annala, PhD; Arion F. Chatziioannou, PhD; Vivekanand Allada, MD; Magnus Dahlbom, PhD; Yuan-Chuan Tai; Masayuki Inubushi, MD; Sung-Cheng Huang, DSc; Simon R. Cherry, PhD; Michael E. Phelps, PhD; Heinrich R. Schelbert, MD Noninvasive Measurement of Myocardial Activity Concentrations and Perfusion Defect Sizes in Rats With a New Small-Animal Positron Emission Tomograph.
12. Guillet B, Quentin P, Waultier S, Bourrelly M, Pisano P, Mundler O. Technologist Radiation Exposure in Routine Clinical Practice with [18F]-FDG PET. *Journal of Nuclear Medicine Technology*. 2005.
13. NC3Rs. The 3Rs. National Centre for the Replacement, Refinement and Reduction of Animals in Research.
14. Taschereau R, Chatziioannou AF. Monte Carlo simulations of absorbed dose in a mouse phantom from 18-fluorine compounds. *Med Phys*. (2007) 34:1026–36. 10.1118/1.2558115
15. Tippayamontri T, Betancourt-Santander E, Guérin B, Lecomte R, Paquette B, Sanche L. Estimation of the Internal Dose Imparted by 18F-Fluorodeoxyglucose to Tissues by Using Fricke Dosimetry in a Phantom and Positron Emission Tomography. *Frontiers in Nuclear Medicine*. 2022.
16. Molinos C, Sasser T, Salmon P, Gsell W, Viertl D, Massey JC, Mińczuk K, Li J, Kundu BK, Berr S, Correcher C, Bahadur A, Attarwala AA, Stark S, Junge S, Himmelreich U, Prior JO, Laperre K, Van Wyk S and Heidenreich M (2019) Low-Dose Imaging in a New Preclinical Total-Body PET/CT Scanner. *Front. Med.* 6:88. doi: 10.3389/fmed.2019.00088
17. Nielsen, C. H., Kimura, R. H., Withofs, N., Tran, P.T., Miao, Z., Cochran, J. R., Cheng, Z., Felsher, D., Kjær, A., Willmann, J. K., & Gambhir, S. S. (2010). PET imaging of tumor neovascularization in a transgenic mouse model with a novel ⁶⁴Cu-DOTA-knottin peptide. *Cancer Research*, 70(22), 9022–9030. <https://doi.org/10.1158/0008-5472.CAN-10-1338>

-
18. Panetta, J., Cvetkovic, D., & Ma, C. M. C. (2018). Comparison of the use of MRI and ¹⁸F-FDG PET/CT in tracking tumor progression and treatment efficacy in mouse models. *International Journal of Radiation Oncology, Biology, Physics*, 102(3 Suppl.), e180.
 19. Kelada, O., Tseng, J.-C., & Peterson, J. (2018). Best practices for preclinical ¹⁸F-FDG PET imaging. *Journal of Nuclear Medicine*, 59(Supplement 1), 1155.
 20. Muller, F. M., Vervenne, B., Maebe, J., Blankemeyer, E., Sellmyer, M. A., Zhou, R., Karp, J. S., Vanhove, C., & Vandenberghe, S. (2023). Image denoising of low-dose PET mouse scans with deep learning: Validation study for preclinical imaging applicability. *Molecular Imaging and Biology*. <https://doi.org/10.1007/s11307-023-01866-x>

Bruker BioSpin
info@bruker.com

bruker.com

Customer Support
[https://www.bruker.com/
en/services/support.html](https://www.bruker.com/en/services/support.html)

Online information
[bruker.com/molecular
imaging](https://www.bruker.com/molecular-imaging)

